






CLINICAL INVESTIGATIVE STUDY

Cortical and white matter lesion topology influences focal corpus callosum atrophy in multiple sclerosis

Michael Platten^{1,2,3}  | Russell Ouellette^{1,2}  | Elena Herranz⁴ | Valeria Barletta⁴  |
 Constantina A. Treaba⁴ | Caterina Mainero⁴ | Tobias Granberg^{1,2} 

¹ Department of Clinical Neuroscience, Karolinska Institutet, Stockholm, Sweden

² Department of Neuroradiology, Karolinska University Hospital, Stockholm, Sweden

³ School of chemistry, biotechnology, and health, KTH Royal Institute of Technology, Stockholm, Sweden

⁴ Division of Multiple Sclerosis Imaging Laboratory, Athinoula A. Martinos Center for Biomedical Imaging and Harvard Medical School, Boston, Massachusetts, USA

Correspondence

Michael Platten, Kungshamra 56A Lgh 1101,
 170 70, Stockholm, Sweden.
 Email: michael.platten@ki.se.

Caterina Mainero and Tobias Granberg are
 co-last authors.

Funding information

COMBAT-MS, Grant/Award Number: (Patient-Centered Outcomes Research Institute grant; National Multiple Sclerosis Society, Grant/Award Number: NMSS 4281-RG-A1 and NMSS RG 4729A2/1; Svenska Sällskapet för Medicinsk Forskning; MultipleMS, Grant/Award Number: (EU Horizon 2020 grant 733161); Erik and Edith Fernström's foundation for medical research; Christer Lindgren and Eva Fredholm Foundation; National Institutes of Health, Grant/Award Number: R01NS078322-01-A1; Region Stockholm and Karolinska Institutet (ALF grant 20150166, 20170036, CIMED junior grant 20190565); U.S. Army, Grant/Award Number: W81XWH-13-1-0122

Abstract

Background and Purpose: Corpus callosum (CC) atrophy is a strong predictor of multiple sclerosis (MS) disability but the contributing pathological mechanisms remain uncertain. We aimed to apply advanced MRI to explore what drives the often nonuniform callosal atrophy.

Methods: Prospective brain 7 Tesla and 3 Tesla Human Connectom Scanner MRI were performed in 92 MS patients. White matter, leukocortical, and intracortical lesions were manually segmented. FreeSurfer was used to segment the CC and topographically classify lesions per lobe or as deep white matter lesions. Regression models were calculated to predict focal CC atrophy.

Results: The frontal and parietal lobes contained the majority ($\geq 80\%$) of all lesion classifications in both relapsing-remitting and secondary progressive MS subtypes. The anterior subsection of the CC had the smallest proportional volume difference between subtypes (11%). Deep, temporal, and occipital white matter lesions, and occipital intracortical lesions were the strongest predictors of middle-posterior callosal atrophy (adjusted $R^2 = .54-.39, P < .01$).

Conclusions: Both white matter and cortical lesions contribute to regional corpus callosal atrophy. The lobe-specific lesion topology does not fully explain the inhomogeneous CC atrophy.

KEYWORDS

atrophy, corpus callosum, magnetic resonance imaging, multiple sclerosis

This is an open access article under the terms of the [Creative Commons Attribution-NonCommercial](https://creativecommons.org/licenses/by-nc/4.0/) License, which permits use, distribution and reproduction in any medium, provided the original work is properly cited and is not used for commercial purposes.

© 2022 The Authors. *Journal of Neuroimaging* published by Wiley Periodicals LLC on behalf of American Society of Neuroimaging.



INTRODUCTION

Multiple sclerosis (MS) is an immune-mediated inflammatory and neurodegenerative disease causing cognitive and physical disability, resulting in high societal costs.¹ The 2017 McDonald diagnostic criteria have increased the role of paraclinical assessments, especially that of imaging in the diagnosis and monitoring of MS.^{2,3}

The corpus callosum (CC) is a large white matter structure composed of commissural fibers connecting the cerebral hemispheres, which can be reliably segmented on 3-dimensional T1-weighted images.⁴ A topological specialization of the CC exists, corresponding to the neuronal interconnectivity of the brain.⁵ A lobe-specific structural connectivity gradient from anterior to posterior within the CC has recently been observed by tractography of 100 healthy subjects.⁶ In a long-term MS follow-up study, the CC was observed as the brain structure with the highest atrophy rate throughout the disease course,⁷ and has been found to be associated with both cognitive and physical disability.⁸ Corpus callosal atrophy has, furthermore, been shown to predict cognitive outcomes in MS,⁷ making it a strategic biomarker to monitor in MS. However, this atrophy does not occur uniformly across the entirety of the CC,⁹⁻¹¹ and we currently do not understand all the potential contributing factors to corpus callosal atrophy. Neurodegeneration, specifically Wallerian degeneration, is believed to be the result of both local and distant inflammation, resulting in atrophy of various structures.¹² It has long been observed that cerebral white matter lesions contribute to CC axonal loss,¹³ and that distant lesions with CC interconnectivity contribute to atrophy via Wallerian degeneration.¹⁴ It is, however, unknown if the lobe-specific lesion burden may explain the uneven topological gradient in CC atrophy. Better understanding this relationship may provide insight into the evolution of neurodegeneration in MS.

Although MS has been considered a white matter disease, ultrahigh-field 7 Tesla (T) MRI has been critical in demonstrating gray matter involvement in vivo, with visualization and characterization of intracortical, leukocortical, and subpial lesions.^{15,16} Cortical lesions have, with 7 T, been found to occur in over 90% of early-stage MS patients.¹⁷ Although the white matter lesion accrual rate is highest among relapsing-remitting MS (RRMS), the cortical lesion accrual rate has been observed to be higher in secondary progressive (SPMS).¹⁸ However, defining the point at which RRMS transitions to SPMS is very difficult due to multiple independent factors. Currently, there are no clear imaging, clinical, or immunologic criteria that define this transition. Practically, this results in a delayed and retrospective diagnosis.¹⁹ Although those with SPMS typically have few new or gadolinium-enhancing white matter lesions, there exists a persistent inflammation coupled with mitochondrial dysfunction that results in axonal damage and ultimately neurodegeneration, including Wallerian degeneration.²⁰ Of note is that the inflammatory and neurodegenerative components of MS are not mutually exclusive but, rather, both exist in early stages of the disease,¹⁷ and evolve at varying relative rates throughout the disease course that, in summation, give rise to the classic disease subtypes defined by current diagnostic criteria.^{21,22} In this

TABLE 1 Cohort demographics

Demographics	Total cohort	RRMS	SPMS
Number of patients	92	66	26
Age, years	43 ± 9.6	42 ± 9.5	47 ± 9.1
Sex (F/M)	69/23	53/13	16/10
Disease duration, years	10 ± 11	7.5 ± 8.8	19 ± 10
EDSS, median, IQR	2.5, 2.0-4.0	2.0, 1.0-3.0	4.5, 4.0-6.0
SDMT z-score	0.0 ± 1.4	0.4 ± 1.0	-1.0 ± 1.4

Note: All the data represent mean ± standard deviation, unless otherwise indicated.

Abbreviations: EDSS, Expanded Disability Status Scale; F/M, female/male; IQR, interquartile range; RRMS, relapsing-remitting multiple sclerosis; SDMT, Symbol Digit Modalities Test; SPMS, secondary progressive multiple sclerosis.

prolific era of treatment development, there exist numerous promising biological and small molecule therapies aiming to promote remyelination and/or provide a neuroprotective effect.²³ Importantly, this is not only for those with RRMS, as for the previous generation of therapies, but also for those in the progressive stages, where neuroregenerative therapies might slow down disability progression.²⁴ Better characterizing the difference between subtypes, such as neurodegeneration via CC atrophy and lesion accumulation, may provide further understanding of this subtype transition, ultimately affecting the choice of therapy.

In this study, we aimed to study the relative contribution of white matter lesions, leukocortical lesions, and intracortical lesions within their respective lobe localization on focal neurodegeneration of the CC. We furthermore evaluated the group-level difference in CC atrophy and lesion load between subtypes in order to explore and discuss how these biomarkers differ across different disease stages.

METHODS

Participants

A cohort of 92 participants, diagnosed with MS according to the McDonald criteria,² was included in this study. Detailed demographics of the cohort are presented in Table 1. As expected, the SPMS subgroup had a longer disease duration and more neurological disability as demonstrated by higher Expanded Disability Status Scale (EDSS) and lower Symbol Digit Modalities Test (SDMT) z-scores normalized based on the age and education level.²⁵

MRI acquisition

All 92 subjects were examined with both 7 T and 3 T brain scans. A Siemens 7 T scanner was used with a custom-built 32-channel phased-array head coil. A 2-dimensional single-echo FLASH T₂*-weighted spoiled gradient-echo pulse sequence was applied (repeti-

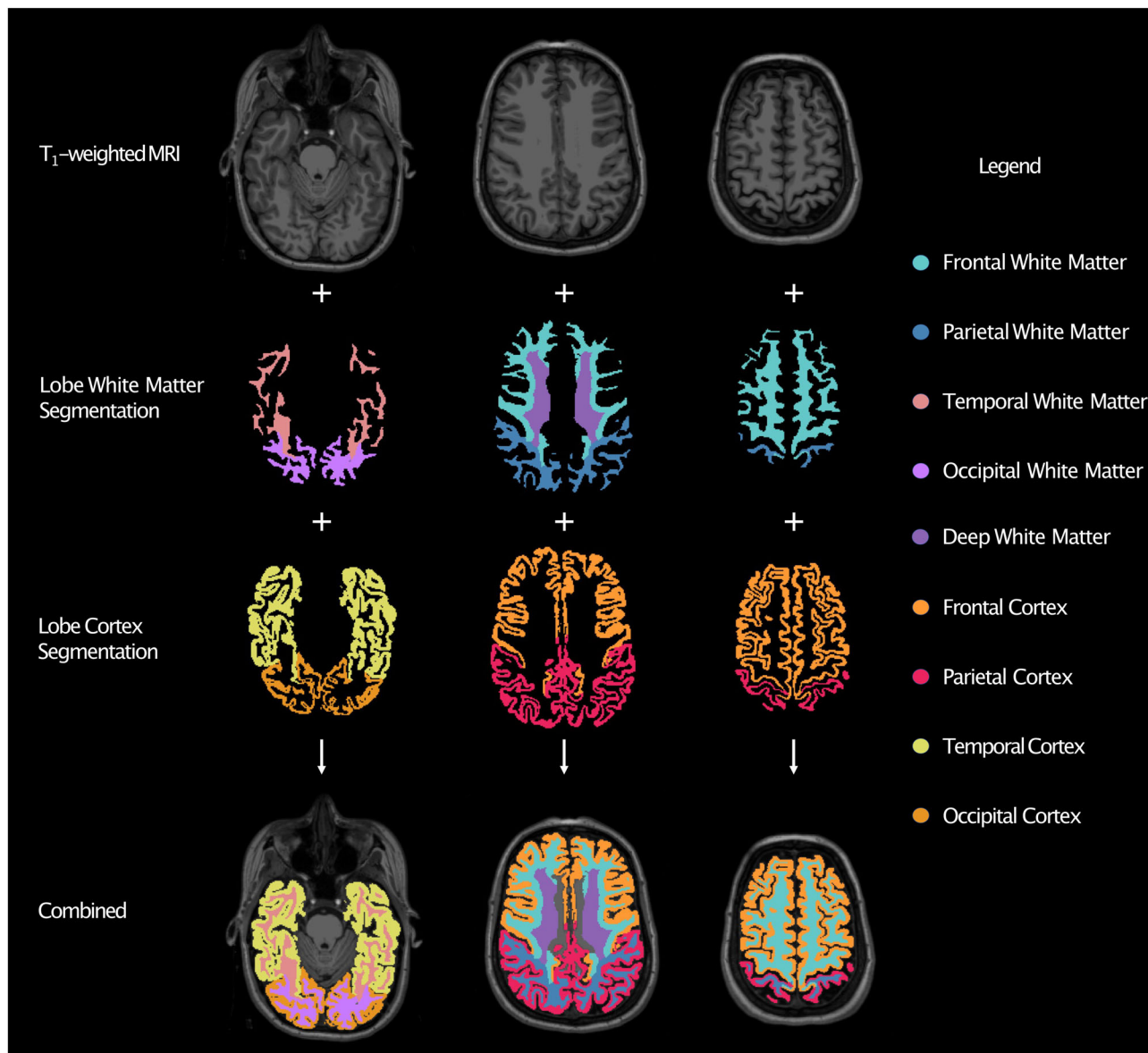


FIGURE 1 Lobe-specific white matter and cortex segmentation pipeline. An example of the output from the pipeline segmenting the white matter and cortex according to frontal, parietal, temporal, and occipital lobes. Additionally, a segmentation of the deep white matter was applied to cover the white matter that was not defined as part of a specific lobe. FreeSurfer 7.0.0 (<http://surfer.nmr.mgh.harvard.edu>, Harvard University, Boston, MA, USA) was used to create the segmentation pipeline.

tion/echo times = 1700/21.8 ms, flip angle 55°, 40 slices each on two separate slabs covering the whole supratentorial brain, field of view = 192 × 168 mm, resolution = 0.33 × 0.33 × 1.0 mm, bandwidth = 335 Hz/pixel, acquisition time for each slab 7:37 minutes). Thereafter, the two slabs were co-registered into FreeSurfer space using a boundary-based registration method. This methodology has been applied and detailed in previous studies.^{26–28}

The 3 T scans were acquired with the MGH-USC Skyra CONNECTOM scanner with a custom-built 64-channel head coil. A 3-dimensional T₁-weighted multi-echo magnetization-prepared rapid gradient-echo (MPRAGE) sequence was acquired for FreeSurfer anatomical reconstructions (repetition/echo/inversion times = 2530/1.15/1100, 3.03, 4.89, 6.75 ms, flip angle 7°, 176 slices, field of

view = 230 × 230 mm, resolution 1.0 × 1.0 × 1.0 mm, bandwidth 651 Hz/pixel, acquisition time 6:02 minutes).

Lobe and corpus callosum segmentation

FreeSurfer 7.0.0 (<http://surfer.nmr.mgh.harvard.edu>, Harvard University, Boston, MA, USA) was used to create the segmentation pipeline.²⁹ The full script applied on this cohort can be found on <https://github.com/plattenmichael/LesionNeurodegeneration>. Figure 1 shows the segmentation of the frontal, parietal, temporal, and occipital cerebral lobes as defined by FreeSurfer's `-lobeStrict` function, using the Desikan-Killiany atlas. As this definition left a substantial amount of

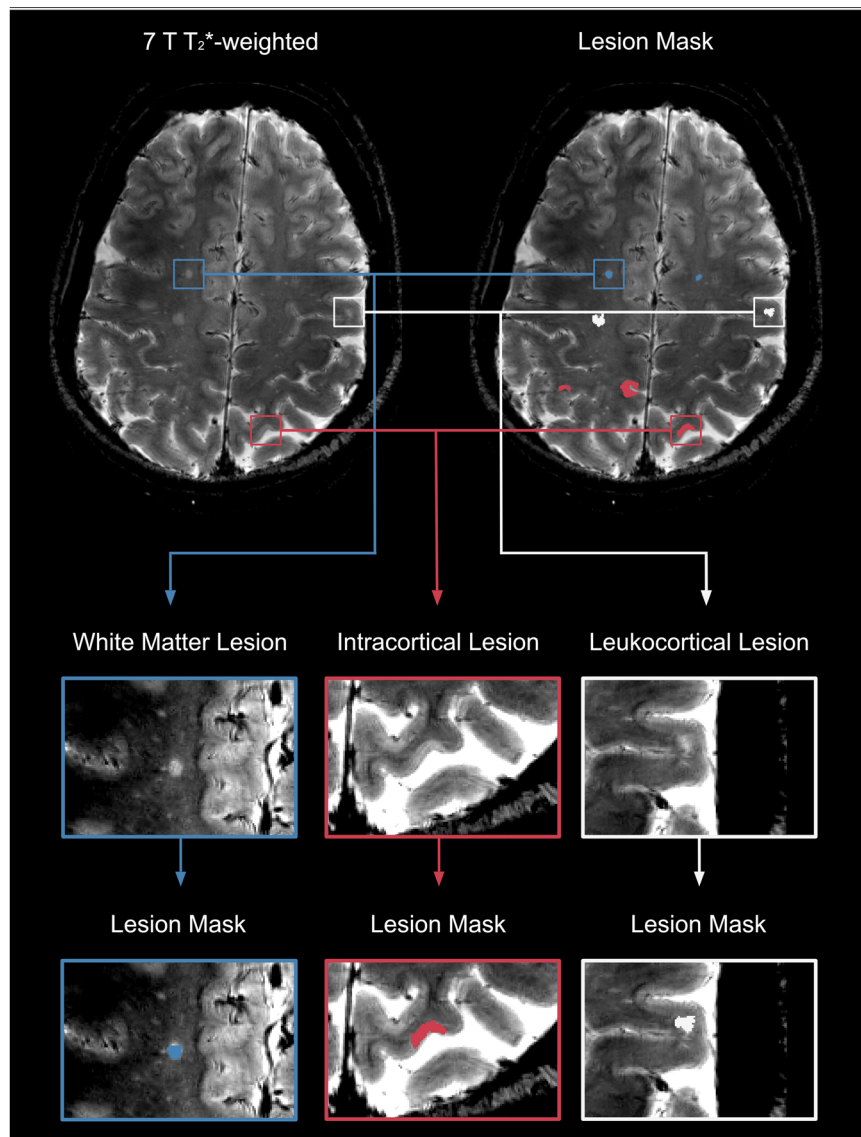


FIGURE 2 Manual segmentation of lesions. All patients underwent a 7 T T_2^* -weighted gradient-echo sequence that was manually segmented by two trained raters. The first rater performed an independent evaluation and segmentation of lesions. The second rater performed quality control of the segmentations. Where there was disagreement, the two raters discussed to find consensus. The lesions appeared as focal hyperintensities and had to extend for at least three voxels and two consecutive slices.

white matter unsegmented, an additional segmentation was added to include the remaining deep white matter not defined as belonging to a specific lobe. The CC was segmented through FreeSurfer's standard subcortical segmentation protocol where the midsagittal slice is located, and the segmentation extends laterally covering a total of 5 mm in width. The segmentation parcellates the CC in five equidistant subsections along its own eigendirection: posterior, mid-posterior, middle, mid-anterior, and anterior.

Lesion quantification

Manual segmentation of cortical lesions was performed, blinded to patients' clinical and demographic data, by agreement of two raters (A.T. and C.M.), using Slicer (v. 4.2.0, <https://www.slicer.org>)³⁰ on the 7 T T_2^* -weighted gradient-echo brain sequence (Figure 2). The first rater performed the initial lesion quantification independently by delineating the lesions. The second rater performed a quality control of all

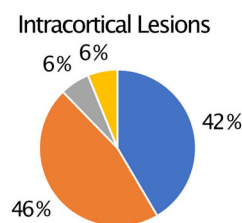
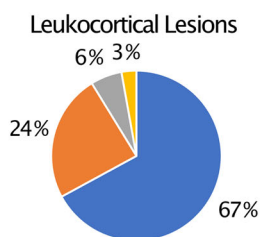
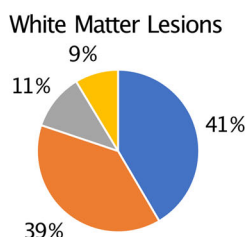
lesion segmentations. Where there was disagreement, consensus was achieved through discussion. The lesions appeared as focal hyperintensities and had to extend for at least three voxels and two consecutive slices. The white matter lesions were segmented by a semi-automated method implemented in Slicer. Both these methods have been applied and detailed previously.²⁸ Brain lesion volumes were extracted using fslstats (FMRIB Software Library, FSL, v. 5.0, Oxford, UK, <http://fsl.fmrib.ox.ac.uk/fsl>).³¹

Statistical analysis

Statistical analyses were performed using SPSS Statistics v. 25.0 for Mac (IBM Corporation, Armonk, NY, USA). Normality was determined by the Shapiro-Wilk test and by evaluation of skewness and kurtosis. Group-level comparisons were performed using independent sample *T*-test and Mann-Whitney *U*-test for parametric and nonparametric data, respectively. Stepwise linear regression analysis was applied for

Lesion Distribution by Lobe

RRMS



SPMS

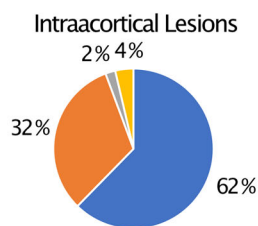
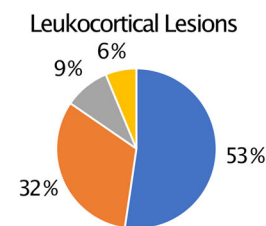
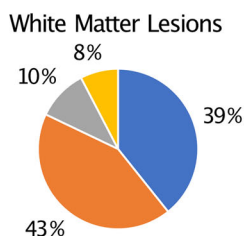


FIGURE 3 Lesion distribution by lobe. The frontal and parietal lobes contained the majority of lesions, of all lesion classifications. Depending on lesion classification, the temporal and occipital lobes jointly accounted for 6%–20% of the total lesion load. RRMS, relapsing-remitting multiple sclerosis; SPMS, secondary progressive multiple sclerosis.

lobe-specific lesion load to predict CC volume. A two-tailed P -value $< .05$ was considered statistically significant.

RESULTS

Lobe-specific lesion load

The parietal and frontal lobes had the largest proportion of lesion volumes of all lesion classifications (Figure 3). The most abundant lesion classification was white matter lesions (Table 2). Patients with SPMS had significantly higher lesion volumes as compared to RRMS, with the exception being intracortical lesion volumes in the temporal and occipital lobes, where no significant difference was noted. The deep white matter segmentation accounted for a large portion of the total white matter lesion load.

Corpus callosum volume

The CC, and all of its subsections, was significantly smaller in participants with SPMS subtype as compared to the RRMS subtype (Figure 4). The largest proportional difference was noted in the mid- to posterior subsections of the CC.

Predictors of corpus callosum atrophy

The best fit models were found for the middle and posterior subsections of the CC (Table 3). The deep white matter lesions, temporal

and occipital white matter lesions, and occipital intracortical lesions were significant predictors for the volume of those CC subsections. The anterior subsections of the CC had relatively weaker models that found the deep white matter lesions, occipital white matter lesions, and temporal leukocortical lesions to be the most significant predictors of atrophy.

DISCUSSION

This study explored the lobe-specific contribution of white matter, leukocortical, and intracortical lesions to the neurodegeneration of the CC in MS. We found that the frontal and parietal lobes contain the largest lesion volumes for all lesion types in both RRMS and SPMS subtypes. The anterior subsection of the CC had the smallest proportional volume difference between subtypes. Stepwise linear regression found the best fit models for the central and posterior portions of the CC, and that the strongest predictors of atrophy were deep white matter, temporal, and occipital white matter lesions, as well as occipital intracortical lesions. However, no clear spatial association was found between lesion location and the CC subsection volumes.

Intracortical lesion distribution with 1.5 T and 3 T scanners has previously found that most intracortical lesions occur in the frontal lobes, followed by the temporal lobes, parietal lobes, and occipital lobes.^{32,33} This is in contrast with our study where we found the order of intracortical lesion abundance to be: frontal, parietal, occipital, and temporal. This difference may be explained by the higher signal and resolution granted by 7 Tesla imaging that allowed capturing of lesions that are

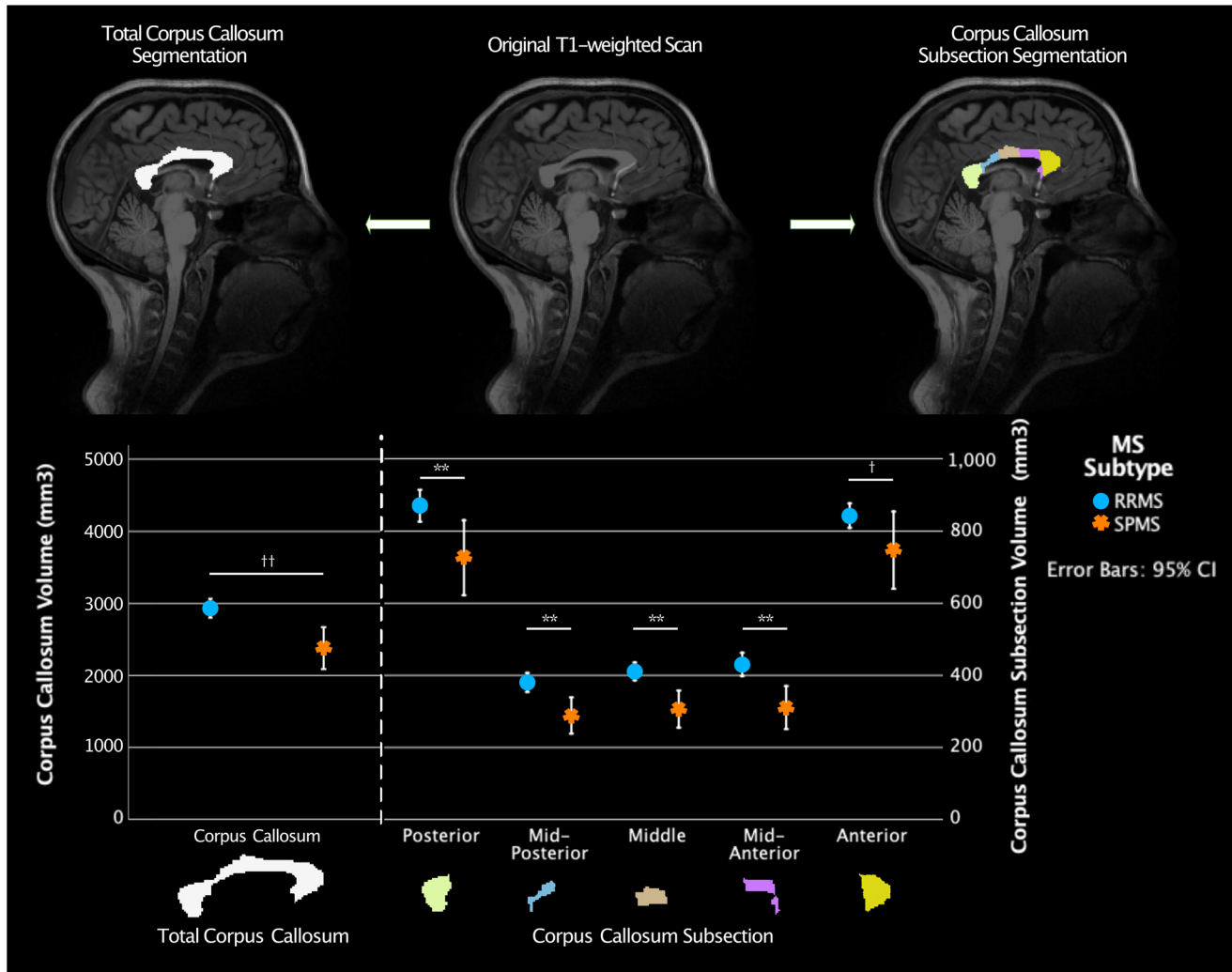


FIGURE 4 Corpus callosum volume difference between multiple sclerosis subtypes. The most significant difference between relapsing-remitting multiple sclerosis and secondary progressive multiple sclerosis exists between the mid and posterior subsections of the corpus callosum. CI, confidence interval; RRMS, relapsing-remitting multiple sclerosis; SPMS, secondary progressive multiple sclerosis. * $P < .05$, by Independent Samples *T*-Test, two-tailed. ** $P < .01$, by Independent Samples *T*-Test, two-tailed. † $P < .05$, by Mann-Whitney *U*-test, two-tailed. †† $P < .01$, by Mann-Whitney *U*-test, two-tailed. Specific test choice was dictated by Levene's test for equality of variance of the respective variables.

more difficult to discern through 1.5 T and 3 T scanners, but larger susceptibility artifacts and more pronounced field inhomogeneities at 7 T could also contribute to the difference. Our finding that the white matter lesion volume was highest in the frontal and parietal lobes is echoed by Sperling et al.³⁴ Similarly, Pandya et al. found higher lesion burden in the frontal and parietal lobes, followed by the temporal and occipital lobes.³⁵ Intracortical gray matter in the frontal and parietal lobe has been observed to significantly atrophy in MS,³⁶ which could possibly be the downstream result of the relative abundance of leukocortical and intracortical lesions found in these lobes in our present study.

The nonuniform atrophy of the CC has previously been described, but the factors contributing to this process are not entirely understood. In a study by van Schependom et al., there was a significantly decreased thickness in the middle portion of the CC in mildly disabled MS patients as compared to healthy controls.¹¹ In a study by

Sigirli et al., the SPMS subtype exhibited greater shape deformation of the CC than RRMS, but both subtypes exhibited significant deformation as compared to healthy controls. Although there was general atrophy, they found that the anterior portion and the trunk of the CC were most strongly affected.¹⁰ In our study, we found the greatest proportional CC volume difference between RRMS and SPMS in the middle and posterior subsections of the CC, which was mostly affected by deep white matter lesions, occipital and temporal white matter lesions, and occipital intracortical lesions. Several studies have presented a topological map of the fibers crossing the CC. Historically this mapping has been achieved through autopsy,⁵ followed by low-resolution DTI,³⁷⁻³⁹ and now most recently through a high-resolution DTI.⁶ The high-resolution study by Archer et al. presents a topological arrangement of tracts where the occipital and temporal lobes cross the posterior/midposterior portion of the CC, the parietal lobes cross



TABLE 2 Lobe-specific lesion volumes by MS subtype

Lesion classification volume (ml)	RRMS (N = 66)	SPMS (N = 26)
Frontal lobe		
White matter	0.57 ± 1.0	2.3 ± 4.5**
Leukocortical	0.21 ± 0.54	0.75 ± 1.4**
Intracortical	0.12 ± 0.19	0.56 ± 1.4*
Parietal lobe		
White matter	0.53 ± 1.0	2.5 ± 3.3**
Leukocortical	0.077 ± 0.18	0.46 ± 0.92**
Intracortical	0.13 ± 0.22	0.29 ± 0.51*
Temporal lobe		
White matter	0.15 ± 0.28	0.60 ± 0.78**
Leukocortical	0.018 ± 0.052	0.13 ± 0.36*
Intracortical	0.017 ± 0.039	0.018 ± 0.029
Occipital lobe		
White matter	0.12 ± 0.24	0.45 ± 0.43**
Leukocortical	0.0093 ± 0.025	0.090 ± 0.18**
Intracortical	0.017 ± 0.049	0.033 ± 0.055
Deep white matter	1.3 ± 1.9	3.4 ± 3.6**
Total white matter	2.7 ± 4.1	9.3 ± 11**
Total leukocortical	0.32 ± 0.69	1.4 ± 2.6**
Total intracortical	0.28 ± 0.42	0.90 ± 1.91*

Note: Values depicted as mean ± standard deviation. N signifies the number of patients.

Abbreviations: RRMS, relapsing-remitting multiple sclerosis; SPMS, secondary progressive multiple sclerosis.

*P < .05, by Independent Samples Test, two-tailed.

**P < .01, by Independent Samples Test, two-tailed.

the posterior/midposterior/middle, and the frontal lobes cross the mid-posterior/middle/midanterior/anterior portions of the CC.⁶ This topological predominance of tracts crossing the posterior, midposterior, and middle portions of the CC provides a theoretical framework that may explain why these subsections exhibit more atrophy and why linear regression of the lobe-specific lesion contribution to atrophy was stronger in these regions. Contrary to the results presented by Sigirli et al., we observed that the anterior subsection of the CC has the smallest percentual volume difference between RRMS and SPMS. This may indicate that neurodegeneration is less prominent in the more anterior portions of the CC during the transition between disease subtypes. Interestingly, we did not find a consistent topological gradient between lesions spanning frontal to occipital in association with the CC, but we did find that deep white matter lesions, those that are closest in proximity to the CC, were consistently one of the stronger predictors of atrophy. The lack of a clear gradient, however, indicates that lesions are not the sole culprit in causing CC atrophy.

There are several limitations to this study that mandate caution with interpretation. Although there exists controversy around what defines a lobe according to the cortex, the line to be drawn for the corresponding lobe's white matter is even less clear. Analogously, the judgment of where the CC begins and ends as you move laterally from the midline is also not readily apparent. In this study, we thus segmented more white matter, termed deep white matter, as a large portion of the white matter lesions were omitted by FreeSurfer's lobe white matter segmentation. This parceling of lobe white matter could potentially result in an underrepresentation of the white matter lesion burden of the "true lobes." It is also intuitive that this deep white matter, which is the white matter closest to the CC, was a consistent predictor of atrophy. Despite these limitations, our study provides an update on the topol-

TABLE 3 Linear regression: Predictors of corpus callosum atrophy

Dependent variable	Independent variables, lesion type	Adjusted R ²	Model F	P-value	Standardized coefficient beta	P-value
Whole corpus callosum	Deep white matter & occipital white matter	.49	44	<.01	-0.47	<.01
					-0.31	<.01
CC posterior	Deep white matter & temporal white matter	.54	54	<.01	-0.43	<.01
					-0.35	<.01
CC mid-posterior	Deep white matter & occipital white matter	.39	30	<.01	-0.43	<.01
					-0.26	.014
CC middle	Temporal white matter & occipital intracortical & deep white matter	.39	20	<.01	-0.35	.018
					-0.18	.030
					-0.29	.048
CC mid-anterior	Deep white matter	.29	39	<.01	-0.55	<.01
CC anterior	Occipital white matter & temporal leukocortical	.20	12	<.01	-0.33	<.01
					-0.22	.33

Abbreviation: CC, corpus callosum.



ogy of white matter, leukocortical, and intracortical lesions in MS. We furthermore provide support for CC atrophy being most strongly predicted by white matter lesions, but that intracortical lesions do play a significant role in contributing to corpus callosal atrophy. These findings highlight that cortical lesions impact MS neurodegeneration, making them a biomarker of interest.

ACKNOWLEDGMENTS AND DISCLOSURE

We would like to thank all the patients and hospital staff for their help in making this study possible. TG is a recipient of the Grant for Multiple Sclerosis Innovation award by Merck, not related. All the other authors declare no conflict of interest.

ORCID

Michael Platten  <https://orcid.org/0000-0001-6297-487X>

Russell Ouellette  <https://orcid.org/0000-0001-9217-1445>

Valeria Barletta  <https://orcid.org/0000-0003-0655-9406>

Tobias Granberg  <https://orcid.org/0000-0001-6700-1022>

REFERENCES

- Filippi M, Bar-Or A, Piehl F, et al. Multiple sclerosis. *Nat Rev Dis Primers* 2018;4:43.
- Thompson AJ, Banwell BL, Barkhof F, et al. Diagnosis of multiple sclerosis: 2017 revisions of the McDonald criteria. *Lancet Neurol* 2018;17:162-73.
- Wattjes MP, Ciccarelli O, Reich DS, et al. 2021 MAGNIMS-CMSC-NAIMS consensus recommendations on the use of MRI in patients with multiple sclerosis. *Lancet Neurol* 2021;20:653-70.
- Van Schependom J, Jain S, Cambron M, et al. Reliability of measuring regional callosal atrophy in neurodegenerative diseases. *Neuroimage Clin* 2016;12:825-31.
- de Lacoste MC, Kirkpatrick JB, Ross ED. Topography of the human corpus callosum. *J Neuropathol Exp Neurol* 1985;44:578-91.
- Archer DB, Coombes SA, McFarland NR, DeKosky ST, Vaillancourt DE. Development of a transcallosal tractography template and its application to dementia. *Neuroimage* 2019;200:302-12.
- Ouellette R, Bergendal Å, Shams S, et al. Lesion accumulation is predictive of long-term cognitive decline in multiple sclerosis. *Mult Scler Relat Disord* 2018;21:110-6.
- Granberg T, Bergendal G, Shams S, et al. MRI-defined corpus callosal atrophy in multiple sclerosis: a comparison of volumetric measurements, corpus callosum area and index. *J Neuroimaging* 2015;25:996-1001.
- Platten M, Brusini I, Andersson O, et al. Deep learning corpus callosum segmentation as a neurodegenerative marker in multiple sclerosis. *J Neuroimaging* 2021;31:493-500.
- Sigirli D, Ercan I, Ozdemir ST, Taskapilioglu O, Hakyemez B, Turan OF. Shape analysis of the corpus callosum and cerebellum in female MS patients with different clinical phenotypes. *Anat Rec* 2012;295:1202-11.
- Van Schependom J, Gielen J, Laton J, et al. The effect of morphological and microstructural integrity of the corpus callosum on cognition, fatigue and depression in mildly disabled MS patients. *Magn Reson Imaging* 2017;40:109-14.
- Lassmann H. Multiple sclerosis pathology. *Cold Spring Harb Perspect Med* 2018;8:a028936.
- Evangelou N, Konz D, Esiri MM, Smith S, Palace J, Matthews PM. Regional axonal loss in the corpus callosum correlates with cerebral white matter lesion volume and distribution in multiple sclerosis. *Brain* 2000;123:1845-9.
- Ciccarelli O, Werring DJ, Barker GJ, Griffin CM, Wheeler-Kingshott CAM, Miller DH, Thompson AJ. A study of the mechanisms of normal-appearing white matter damage in multiple sclerosis using diffusion tensor imaging—evidence of Wallerian degeneration. *J Neurol* 2003;250:287-92.
- Mainero C, Benner T, Radding A, van der Kouwe A, Jensen R, Rosen BR, Kinkel RP, et al. In vivo imaging of cortical pathology in multiple sclerosis using ultra-high field MRI. *Neurology* 2009;73:941-8.
- Stadelmann C, Albert M, Wegner C, Brück W. Cortical pathology in multiple sclerosis. *Curr Opin Neurol* 2008;21:229-34.
- Granberg T, Fan Q, Treaba CA, et al. In vivo characterization of cortical and white matter neuroaxonal pathology in early multiple sclerosis. *Brain* 2017;140:2912-26.
- Treaba CA, Granberg TE, Sormani MP, et al. Longitudinal characterization of cortical lesion development and evolution in multiple sclerosis with 7.0-T MRI. *Radiology* 2019;291:740-9.
- Inojosa H, Proschmann U, Akgün K, Ziemssen T. A focus on secondary progressive multiple sclerosis (SPMS): challenges in diagnosis and definition. *J Neurol* 2021;268:1210-21.
- Klineova S, Lublin FD. Clinical course of multiple sclerosis. *Cold Spring Harb Perspect Med* 2018;8(9):a028928.
- Lassmann H. Pathogenic mechanisms associated with different clinical courses of multiple sclerosis. *Front Immunol* 2018;9:3116.
- Lucchinetti CF, Popescu BFG, Bunyan RF, et al. Inflammatory cortical demyelination in early multiple sclerosis. *N Engl J Med* 2011;365:2188-97.
- Piehl F. Current and emerging disease-modulatory therapies and treatment targets for multiple sclerosis. *J Intern Med* 2021;289:771-91.
- Goldschmidt C, McGinley MP. Advances in the treatment of multiple sclerosis. *Neurol Clin* 2021;39:21-33.
- Lezak MD, Howieson DB, Bigler ED, et al. *Neuropsychological assessment*. Oxford, New York: Oxford University Press; 2012.
- Greve DN, Fischl B. Accurate and robust brain image alignment using boundary-based registration. *Neuroimage* 2009;48:63-72.
- Louapre C, Govindarajan ST, Gianni C, et al. Heterogeneous pathological processes account for thalamic degeneration in multiple sclerosis: insights from 7 T imaging. *Mult Scler* 2018;24:1433-44.
- Mainero C, Louapre C, Govindarajan ST, et al. A gradient in cortical pathology in multiple sclerosis by in vivo quantitative 7 T imaging. *Brain* 2015;138:932-45.
- Reuter M, Schmansky NJ, Rosas HD, Fischl B. Within-subject template estimation for unbiased longitudinal image analysis. *Neuroimage* 2012;61:1402-18.
- Fedorov A, Beichel R, Kalpathy-Cramer J, et al. 3D Slicer as an image computing platform for the quantitative imaging network. *Magn Reson Imaging* 2012;30:1323-41.
- Jenkinson M, Beckmann CF, Behrens TEJ, Woolrich MW, Smith SM. FSL. *Neuroimage* 2012;62:782-90.
- Curti E, Graziuso S, Tsantes E, Crisi G, Granella F. Correlation between cortical lesions and cognitive impairment in multiple sclerosis. *Brain Behav* 2018;8:e00955.
- Calabrese M, Battaglini M, Giorgio A, et al. Imaging distribution and frequency of cortical lesions in patients with multiple sclerosis. *Neurology* 2010;75:1234-40.
- Sperling RA, Guttman CRG, Hohol MJ, et al. Regional magnetic resonance imaging lesion burden and cognitive function in multiple sclerosis: a longitudinal study. *Arch Neurol* 2001;58:115-21.
- Pandya S, Kaunzner U, Rua SMH, et al. Impact of lesion location on longitudinal myelin water fraction change in chronic multiple sclerosis lesions. *J Neuroimaging* 2020;30:537-43.
- Han X, Tian H, Han Z, et al. Correlation between white matter damage and gray matter lesions in multiple sclerosis patients. *Neural Regen Res* 2017;12:787-94.



37. Hofer S, Frahm J. Topography of the human corpus callosum revisited—comprehensive fiber tractography using diffusion tensor magnetic resonance imaging. *Neuroimage* 2006;32:989-94.
38. Huang H, Zhang J, Jiang H, et al. DTI tractography based parcellation of white matter: application to the mid-sagittal morphology of corpus callosum. *Neuroimage* 2005;26:195-205.
39. Pannek K, Mathias JL, Bigler ED, Brown G, Taylor JD, Rose S. An automated strategy for the delineation and parcellation of commissural

pathways suitable for clinical populations utilising high angular resolution diffusion imaging tractography. *Neuroimage* 2010;50:1044-53.

How to cite this article: Platten M, Ouellette R, Herranz E, et al. Cortical and white matter lesion topology influences focal corpus callosum atrophy in multiple sclerosis. *J Neuroimaging*. 2022;32:471–479. <https://doi.org/10.1111/jon.12977>